PCCP

Accepted Manuscript




ROYAL SOCIETY OF CHEMISTRY

www.rsc.org/pccp

Journal Name

ARTICLE

# Exploring Environment-dependent effects of Pd nanostructures on reactive oxygen species (ROS) using electron spin resonance (ESR) technique: implications for biomedical applications

Received 00th January 20xx,
Accepted 00th January 20xx

DOI: 10.1039/x0xx00000x

www.rsc.org/

Tao Wen,[abd] Weiwei He,[bc] Yu Chong,[b] Yi Liu,[b] Jun-Jie Yin*[b] and Xiaochun Wu*[a]

Recently, because of the great advances in tailoring their shape and structure, palladium nanoparticles (Pd NPs) are receiving increasing attention in biomedical fields apart from their traditional applications as industrial catalysts. When considering the potential uses of Pd NPs in biomedicine, their catalytic properties need to be evaluated under physiologically relevant conditions. In this article, we demonstrate that Pd nanostructures (NSs, both commercial Pd NPs and in–house–prepared Au@Pd nanorods) can induce $O_2$ or •OH production dependent on pH values in the presence of $H_2O_2$. We observed that $O_2$ is produced under neutral and alkaline conditions but •OH under acidic conditions. We also found that Pd NSs can scavenge superoxide and singlet oxygen, which may provide protection in biological systems. On the other hand, their oxidase-like activity may accelerate the oxidation of ascorbic acid and thus may produce negative biological effects. The presented study will provide useful guidance for designing noble metal nanostructures with desired catalytic and biological properties in biomedical applications.

## Introduction

Palladium (Pd) is a common metal with remarkable catalytic, mechanic and electronic properties. It is used in industrial processes and even medicine fields, such as dental appliances.[1] With the development of nanoscience, Pd nanostructures (Pd NSs) have gained plenty of interest in the last decade. Unlike the other noble metal nanoparticles (gold, silver and platinum), the research of Pd NSs in biomedical field is rare. For example, Docherty et al. investigate the size-dependence antimicrobial activity of Pd nanoparticles (NPs).[2] Gómez-Ruiz et al reported that Pd NPs supported on mesoporous silica displayed high cytotoxic activity against four tested human cancer cell lines.[3] However, there have been many advances in the synthesis of Pd NSs with a rich variety of controlled shapes. These materials are made possible through fabrication methods including oxidative etching,[4-6] surface capping,[7] kinetic control, thermodynamic control[8] and so on.[9] As an excellent property for noble metal NSs, most of the chemically synthesized Pd NSs exhibit localized surface plasmon resonance (SPR) in the UV and visible spectral regions. Thus localized SPR enhanced catalysis can only be explored in this spectral region where interferences with endogenous chromophores greatly limit biomedical applications.[10] Recently, with the pioneering work of Zheng et al. in obtaining hexagonal Pd nanosheets, a strong and tunable SPR band in the near-infrared (NIR) spectral region have been obtained for Pd NSs.[7] This work opens a door for applications in biomedicine by utilizing Pd NSs with SPR in NIR region.[11-15]

A very interesting observation for many nanomaterials is that they can promote the formation of reactive oxygen species (ROS), which are most frequently associated with NS-associated toxicities.[16] ROS, such as hydrogen peroxide ($H_2O_2$), hydroxyl radicals (•OH), superoxide ($O_2^{\bullet-}$), and singlet oxygen ($^1O_2$), are the byproducts of normal intracellular metabolism, and they play key physiological roles in cells and tissues. However, overproduction of these ROS can cause oxidative stress and in turn produce adverse effects,[17, 18] such as damage of DNA, lipid peroxidation, and a resulting pathogenic response. Apart from influencing the types and levels of ROS, nanomaterials may influence the antioxidant defense system and cause organism damage. For example, ascorbic acid, a commonly used antioxidant, can protect the organism from oxidation. Pt NSs with ascorbic acid oxidase (AAO) activity have been found to scavenge AA effectively. In addition, our previous theoretical simulation indicates that Pd has a peroxidase activity similar to that of Pt.[19] When considering the potentials for use of Pd NSs in biomedicine, their interactions with ROSs and influences need to be considered carefully under physiologically relevant conditions.

[a] CAS Key Laboratory of Standardization and Measurement for Nanotechnology, National Center for Nanoscience and Technology, Beijing 100190, P. R. China.
[b] Division of Analytical Chemistry, Office of Regulatory Science, Center for Food Safety and Applied Nutrition, US Food and Drug Administration, College Park 20740, MD, USA.
[c] Key Laboratory of Micro-Nano Materials for Energy Storage and Conversion of Henan Province, Institute of Surface Micro and Nano Materials, Xuchang University, Henan 461000, P. R. China.
[d] University of the Chinese Academy of Sciences, Beijing 100190, P. R. China.

† Electronic Supplementary Information (ESI) available: Details of experimental section and figures, See DOI: 10.1039/b000000x/

Electron spin resonance (ESR) spectroscopy is a direct and reliable method to identify and quantify reactive intermediates with unpaired electrons in both chemical and biological environments. ESR technique is proved to be a reliable technique to characterize and identify transient radical intermediates such as reactive oxygen species (•OH, $O_2^{\bullet-}$, $^1O_2$ etc) related to nanomaterials.[20, 21] For instance, we have investigated the effects of Au, Ag, and Pt nanoparticles (NPs) on ROS using ESR technique.[22-24] What is the effect of Pd on ROS? In the current study, we examine the interactions between Pd NSs and $H_2O_2$ at different pHs, and the interaction of Pd NSs with $O_2^{\bullet-}$ and $^1O_2$. With the help of ESR spin trap and spin label techniques, we also investigate the intrinsic activity of Pd NSs to catalyze the oxidation of the antioxidant AA. This study provides a model system for understanding the biological effects of Pd NSs under physiologically relevant conditions.

## Materials and methods

### Chemical and materials

Pd coated Au nanorods (Au@Pd NRs) with aspect ratio of ~ 3.3 and coated with polystyrenesulfonate (PSS) were prepared according to reported methods.[25] 5-tert-Butoxycarbonyl-5-methyl-1-pyrroline N-oxide (BMPO) was purchased from Bioanalytical Labs (Sarasota, FL). 4-Oxo-2,2,6,6-tetramethylpiperidine-d16-1-oxyl ($^{15}$N-PDT) was purchased from Cambridge Isotope Labs (Andover, MA). 1-Hydroxy-3-carboxy-2,2,5,5-tetramethylpyrrolidine- hydrochloride (CPH) was purchased from Alexis, Enzo Life Sciences, Inc. (NY, USA). Hydrogen peroxide ($H_2O_2$, 30%), 3-carbamoyl-2,5-dihydro-2,2,5,5-tetramethyl-1H-pyrrol-1-yloxyl (CTPO), dimethyl sulfoxide (DMSO), diethylenetriaminepentaacetic acid (DTPA), xanthine (Xan), xanthine oxidase (XOD), superoxide dismutase (SOD), 2,2,6,6-tetramethyl-4-piperidine (TEMP), sodium azide ($NaN_3$), ascorbic acid (AA), ascorbic acid oxidase (AAO), palladium powder (Pd NPs, <25 nm) and standard buffer solutions were all purchased from Sigma-Aldrich (St. Louis, MO). The concentration of buffer stock solution (pH 1.09 HCl–KCl, pH 3.9 HAc–NaAc, pH 7.4 PBS, pH 9.4 PBS, pH 10.9 HCl–KOH) was fixed to 0.1 M. Before use, each buffer was treated with Chelex100 molecular biology grade resin from Bio-Rad Laboratories (Hercules, CA) to remove trace metal ions. Milli-Q water (18 MΩ cm) was used for preparation of all solutions.

The concentration unit of commercial Pd NPs is “μg/mL”, used as it marked, and the unit of rod-shape Au@Pd core-shell nanorods (NRs) synthesized by ourselves (NRs with ca. 64 nm long and aspect ratio of ~3.3) is “nM”, usually counted by nanorod concentration. The “nM" is used here to make it easier when comparison to gold nanorod with similar shape and the same nanorod concentration but different element. The weight ratio of Pd to Au (Pd/Au) is 0.163, obtained using EDX.

### Characterization

UV-Vis absorption spectra were obtained using a Varian Cary 300 spectrophotometer. Transmission electron microscopy (TEM) images were captured on a JEM 2100 FEG (JEOL) transmission electron microscope (accelerating voltage of 200 kV). Scanning transmission electron microscopy (STEM) and energy-dispersive X-ray analysis (EDX) element mappings were conducted with a Tecnai $G^2$ F20 U-Twin microscope. The samples for TEM, STEM analysis were prepared by adding drops of the redispersed colloidal solutions onto standard holey carbon-coated copper grids, which were then air dried at room temperature.

### Kinetic parameters using UV-Vis spectroscopy

The oxidation of AA catalyzed by ascorbic acid oxidase (AAO) or Pd NSs in buffers was performed at 22°C as follows: AA was mixed with buffers. Then, sufficient AAO or Pd NSs (or Au NRs) were added. The reaction kinetics for the catalytic oxidation of AA was studied by recording the absorption spectra of solutions with a total volume of 1 mL. Data were collected at 1 min intervals with the spectrophotometer in the scanning kinetics mode. The oxidation of AA was monitored by measurement of its absorbance at the $\lambda_{max}$ (265 nm).

### Electron spin resonance

All ESR measurements were carried out using a Bruker EMX ESR spectrometer (Billerica, MA) at ambient temperature. 50 μL aliquots of control or sample solutions were put in glass capillary tubes with internal diameters of 1 mm and sealed. For samples with light irradiation, sealed quartz capillary tubes with internal diameters of 0.9 mm were used. The capillary tubes were inserted into the ESR cavity and the spectra were recorded at selected times. Other settings were as follows: 1 G field modulation, 100 G scan range, and 20 mW microwave power for detection of •OH, $O_2^{\bullet-}$, and $^1O_2$. For ESR oximetry using the spin probe, $^{15}$N-PDT, and the instrument settings were: 0.05 G field modulation, 2 G scan range, and 1 mW microwave power. For ESR oximetry using CTPO, instrument settings were: 0.04 G field modulation, 5 G scan range, and 1 mW microwave power.

The spin trap, BMPO, was used to identify •OH formed during the degradation of $H_2O_2$ in the presence of Pd NSs

Journal Name

ARTICLE

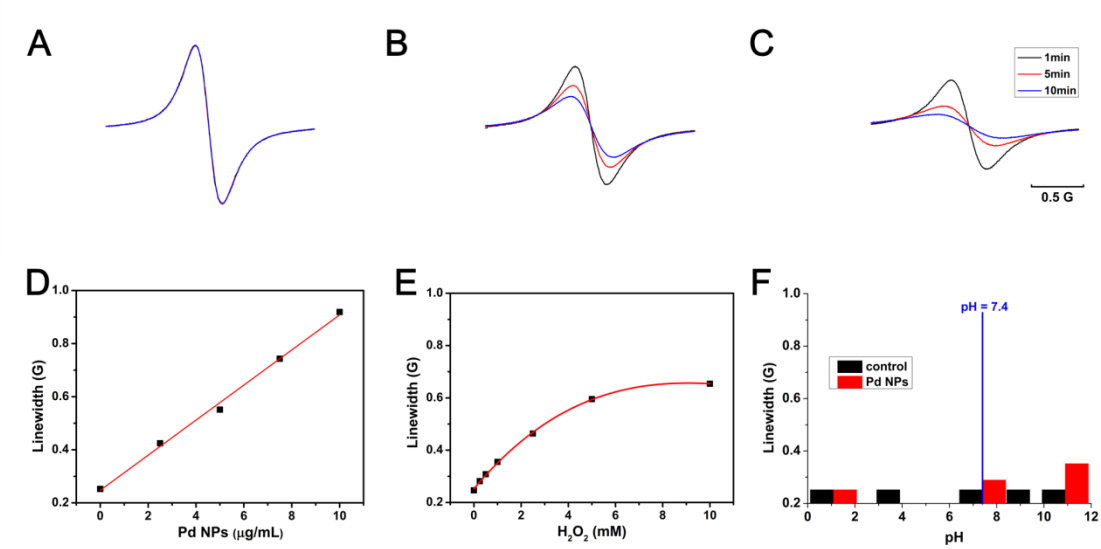


Fig. 1 ESR spectra of 0.2 mM $^{15}$N-PDT in the presence of 2.5 μg/mL Pd NPs, 10 mM buffer, and 5 mM $H_2O_2$ at different time intervals at different pH values: (A) pH 1.09, (B) pH 7.4, (C) pH 10.9. (D) Effect of Pd NPs concentration at 10 mM buffer (pH 7.4) with 5mM $H_2O_2$ after incubation for 1 min. (E) Effect of $H_2O_2$ concentration at 10 mM buffer (pH 7.4) and 2.5 μg/mL Pd NPs after incubation for 10 min. (F) Effect of pH on line width for Pd NPs after incubation for 1 min. The solutions contain 10 mM buffer, 0.2 mM $^{15}$N-PDT, 5 mM $H_2O_2$ and 2.5 μg/mL Pd NPs.

under various conditions. The amount of •OH is quantitatively estimated by the ESR signal intensity of the hydroxyl radical spin adduct (BMPO/•OH) using the peak-to-peak height of the second line of the ESR spectrum. The $H_2O_2$ solution was mixed with BMPO in buffer solutions with different pHs and the reaction was initiated by adding Pd NSs.

For ESR oximetry experiments, 0.2 mM $^{15}$N-PDT was mixed with different concentrations of buffered $H_2O_2$ solutions containing Pd NSs. To investigate the consumption of oxygen during oxidation of AA, 0.1 mM CTPO was mixed with Pd NSs ([Pd NPs] = 100 μg/mL and [Au@Pd NRs] = 2.5 nM), and 5 mM AA in 10 mM PBS buffer (pH = 7.4).

To examine the ability of Pd NSs to scavenge $O_2^{\bullet-}$, Xan/XOD was used to generate $O_2^{\bullet-}$ in PBS buffer (10 mM, pH 7.4). 25 mM BMPO was used to trap $O_2^{\bullet-}$ by forming the spin adduct, BMPO/•OOH. The reaction was started by the addition of XOD. The other concentrations are: [Xan] = 1 mM, [XOD] = 0.05 U/mL, and [DTPA] = 0.05 mM.

To investigate the interaction between $^1O_2$ and Pd NSs, $^1O_2$ was produced by irradiating 0.02 mg/mL ZnO with a 450 W Xenon lamp coupled to 340 nm band pass filter. 10 mM TEMP was used to trap $^1O_2$ to form TEMPONE. The reaction was started by irradiation.

To further distinguish ROS, DMSO, SOD and $NaN_3$ were employed separately to test their scavenging effect on the ESR signal for hydroxyl radical, superoxide and singlet oxygen, respectively.

Stock solutions of CPH were prepared shortly before use. To investigate the oxidation of CPH by Pd NSs, 0.1 mM CPH was mixed with different concentrations of Pd NSs and the reaction was initiated by adding Pd NSs.

## Results and discussion

### Generation of oxygen during decomposition of $H_2O_2$ under neutral and alkaline conditions

The dispersity of Pd NPs is not good but commercially used (see TEM images in Fig. S1†). Pd NPs were found to exhibit pH-dependent catalase like activities (Fig. 1). $O_2$ bubbles were visually observed in closed capillary tubes containing $H_2O_2$ and Pd NPs at pHs ranging from 7.4 to 10.9. No bubbles are seen in the control samples with only $H_2O_2$ (Fig. S3†). The generation of $O_2$ was monitored using ESR oximetry in conjunction with the spin probe $^{15}$N-PDT.[26] The bimolecular collision of paramagnetic $O_2$ and the spin probe leads to spin exchange, resulting in shorter relaxation times for the spin probe. Thus,

ESR signals of the spin probe get broader. The broadening of the spin probe's ESR signal indicates the concentration of oxygen, so the changes of line width (LW) can be used to show changes in the concentration of oxygen. In the absence of nanomaterials, there is no change in the LW of $^{15}$N-PDT in the absence or presence of $H_2O_2$ as the solution pH values are changed from 1.09 to 10.9 (Fig. S4†). After adding Pd NPs, the LW shows no change at pH = 1.09, but becomes broader when solution pH values increase to 7.4 and higher. Higher pHs lead to larger LW. When increasing Pd NPs concentration, a linear increase in LW versus particle concentration (< 10 μg/mL) is observed (Fig. 1D). At low $H_2O_2$ concentrations, LW rapidly increases. At high $H_2O_2$ concentrations, the LW increase tends to saturation (Fig. 1E). For rod-shaped Au@Pd NRs, which have SPR in NIR region and could bring in much more potential applications, is pretty uniform (Fig. S1†). They have similar pH dependent catalytic behaviour is observed (Fig. S5†). However, Au NR cores show negligible catalase-like activity from pH 1.09 to 10.9, indicating Pd is more effective than Au in catalyzing the disproportion reaction of $H_2O_2$. From UV-Vis spectra, we didn't observe obvious difference with time, showing that Pd NSs (Pd NPs and Au@Pd NRs) have catalase-like activity at neutral and alkaline conditions.

Catalase is a common enzyme found in living organisms exposed to oxygen. Due to its specificity to $H_2O_2$, catalase has wide applications, such as anti-aging therapy, fabrication of biosensors, and in food processing. It has also been recognized as an antioxidant enzyme due to its ability to catalyze the decomposition of $H_2O_2$, thus protecting cells and tissues from oxidative damage. Due to the effect on the decomposition of $H_2O_2$, Pd NSs may be also useful as catalase mimetics in any applications involving decomposition of $H_2O_2$ because of their lower cost and easy preparation.

**Generation of hydroxyl radicals with $H_2O_2$ under acidic condition**

Hydroxyl radicals (•OH), one of the most reactive and damaging ROS, can be detected by ESR with the help of a spin trap. •OH can readily react with diamagnetic nitrone spin traps and form a stable free radical (spin adduct), which can be identified from its ESR spectrum. Here we employ BMPO as the spin trap to specifically detect short-lived •OH as the spin adduct, BMPO/•OH. The ESR spectrum for the spin adduct BMPO/•OH has four lines with relative intensities of 1:2:2:1 and hyperfine splitting parameters of $a_N$= 13.56, $a_H^\beta$ = 12.30, $a_H^\gamma$= 0.66.[27] This characteristic spectrum is observed in samples containing Pd NPs and $H_2O_2$ at pH 1.09 (Fig. 2). DMSO is an efficient and specific scavenger for •OH. As Fig. 2A shows, in the presence of DMSO, the ESR signal intensity of BMPO/•OH reduces greatly, supporting that the signal comes from •OH. Generation of •OH is highly dependent on pH. To better define the conditions for the formation of •OH, we examined the generation of •OH over a wide pH range (Fig. 2B). As we previously noted, between pH 7.4 and 10.9, oxygen is formed during the decomposition of $H_2O_2$ facilitated by Pd NPs. Here we note that no •OH signals are detected in this pH range. Only under acidic condition (pH 1.09 and 3.9), are •OH signals observed. The signal for BMPO/•OH obtained at pH 1.09 is much larger than that obtained at pH 3.9. These results indicate that pH plays a key role in the catalytic behaviour and an acidic environment is required for generating •OH. For Au@Pd NRs, they show a similar pH dependent •OH production trend (Fig. S6†). Au NRs cores didn't exhibit significant catalase-like behaviour at neutral and alkaline conditions, while they do plays a role in producing •OH at strongly acidic conditions. A Fenton-like mechanism might be responsible for the generation of •OH in the presence of Pd

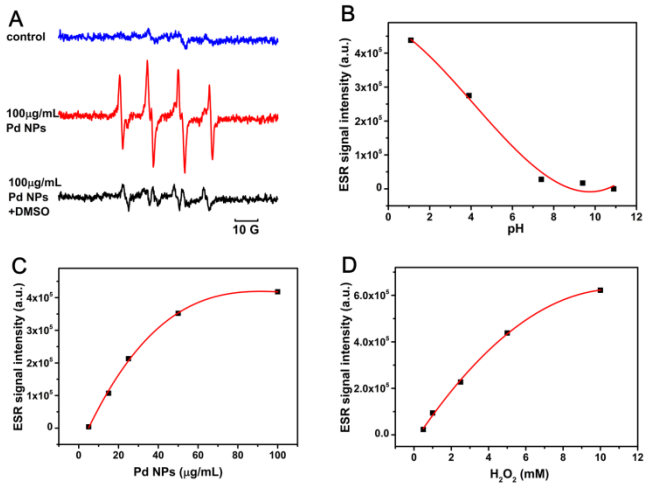


Fig. 2 (A) ESR spectra of BMPO/•OH adducts obtained from samples containing 10 mM buffer (pH 1.09), 5 mM $H_2O_2$ and 25 mM BMPO. (B) Effect of pH on the generation of •OH. The solutions contain 25 mM BMPO, 100 μg/mL Pd NPs, 5 mM $H_2O_2$ and 10 mM different pH buffers. (C) Effect of Pd NPs concentration on the generation of •OH. The solutions contain 25 mM BMPO, 5 mM $H_2O_2$, 10 mM buffer (pH 1.09), and different concentrations of Pd NPs. (D) Effect of $H_2O_2$ concentration on the generation of •OH. The solutions contain 25 mM BMPO, 100 μg/mL Pd NPs, 10 mM buffer (pH 1.09), and different concentrations of $H_2O_2$. ESR spectra were collected after 1 min of incubation and averaged from 9 scans.

Journal Name

ARTICLE

NSs under acidic conditions (Fig. S7 and S8†), which is similar to the mechanism of generation •OH by Ag NPs.[23]

As is known, •OH are extremely reactive and can cause oxidative damage to lipids, proteins, DNA and amino acids. The generation of •OH induced by Pd NSs at acidic conditions illustrates that the acidic conditions of microenvironments in biological systems could have detrimental effect in biomedical applications involving Pd NSs.

**Interaction with superoxide: SOD like activity**

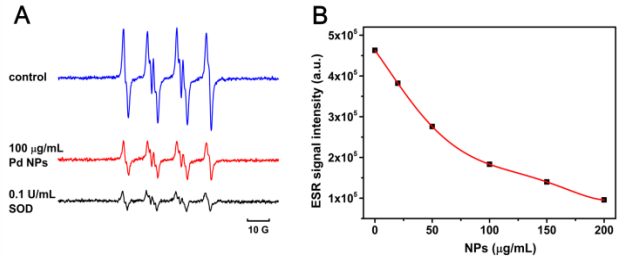


Fig. 3 SOD-like activity of Pd NSs in scavenging superoxide. (A) ESR spectra of BMPO/•OOH adducts obtained from samples containing Pd NPs or SOD. (B) Effect of Pd NPs concentration on their $O_2^{\bullet-}$ scavenging activity. ESR spectra were collected after incubation with BMPO (25 mM) for 5 min in XOD system containing 1 mM Xan, 0.05 U/mL XOD, 0.05 mM DTPA, and 10 mM PBS buffer (pH 7.4).

It is well known that superoxide dismutase (SOD) can catalyze the dismutation of superoxide into oxygen and hydrogen peroxide, and that SOD is very important for antioxidant defenses in cells. To investigate the interaction with $O_2^{\bullet-}$, we find that Pd NPs can scavenge $O_2^{\bullet-}$. To verify this, we generated superoxide using the xanthine/xanthine oxidase system (Xan/XOD).[28] The spin trap BMPO was chosen as it can form a spin adduct with superoxide (designated BMPO/•OOH). The ESR spectral characteristics of BMPO/•OOH show four lines with relative intensities of 1:1:1:1, and two hyperfine splitting parameters, $a_N$ = 13.4 and $a_H^\beta$ = 12.1 (Fig. 3A).[29]

Superoxide is generated by Xan/XOD under neutral conditions to maximize the activity of XOD. The ESR signal intensity of BMPO/•OOH gradually reduces with increasing the concentration of Pd NPs (Fig. 3B). These data indicate that Pd NPs can scavenge $O_2^{\bullet-}$ in a concentration-dependent manner. Similar concentration-dependent effects are observed in Au NRs and Au@Pd NRs (Fig. S9). Au@Pd NRs have a higher scavenging effect than Au NRs.

As an important antioxidant enzyme with a high specificity for $O_2^{\bullet-}$, SOD can maintain a balance of ROS in an organism and protect cellular components against oxidative damage caused by superoxide. Similar to Au and Pt NPs,[22, 24] Pd NSs can also serve as an alternative mimetic for SOD.

**Interaction with singlet oxygen**

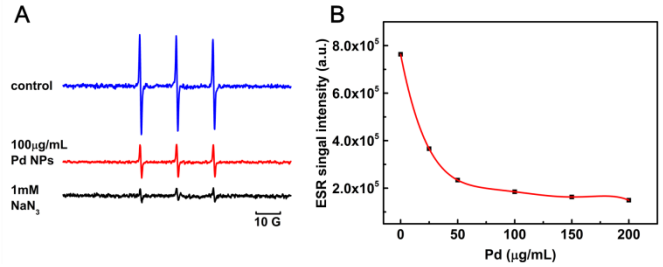


Fig. 4 (A) ESR spectra of TEMPONE from samples containing 10 mM TEMP, 0.02 mg/mL ZnO and 100 μg/mL Pd NPs or 1 mM $NaN_3$ as noted. (B) Effect of Pd NPs concentration on their $^1O_2$ scavenging activity. All the spectra were recorded during irradiation with a Xenon lamp coupled to 340 nm band pass filter for irradiation 1 min.

Singlet oxygen ($^1O_2$) is another important ROS, which is relevant to many oxidation reactions. Singlet oxygen is a powerful oxidant and is toxic to cells. Recently, noble metal NSs, such as Au, Ag, Pt and Pd, have been reported to enable the generation of singlet oxygen upon localized SPR excitation.[30-34] Among these NSs, Pd NPs are regarded as the most effective for $^1O_2$ generation. $^1O_2$ is even obtained from Pd nanocubes without localized SPR excitation.[35] In a recent report, the authors call this kind of singlet oxygen-like species as singlet-$O_2$-analogous species, which have properties similar to $^1O_2$.[36] This research indicates that the relationship between noble metal nanostructures (such as Pd NSs) and $^1O_2$ is complex.

$^1O_2$ can be produced by irradiating rose bengal with visible light or certain metal oxides, including $TiO_2$ and ZnO, with UV light.[37] Here, ZnO NPs are used to photosensitize the generation $^1O_2$ during exposure to 340 nm light. 2,2,6,6-Tetramethyl-4-piperidine (TEMP) was used as a spin trap to study the effect of Pd NPs. The spin trap, TEMP, can specifically capture $^1O_2$ to yield a nitroxide radical (4-oxo-2,2,6,6-tetramethylpiperidine-N-oxyl, TEMPONE) with a stable ESR signal. ESR spectra for TEMPONE characteristically have three lines with equal intensities, with a hyperfine splitting parameter of $a_N$ = 16.0.[38, 39] A well-known $^1O_2$ scavenger, $NaN_3$, was employed to show the effects of scavenging under these experimental conditions. As Fig. 4A shows, after adding Pd NPs, the ESR signal intensity of TEMPONE dramatically reduces, in a manner similar to that seen when $NaN_3$ is added. This demonstrates that Pd NPs can scavenge $^1O_2$. The ESR

Journal Name

ARTICLE

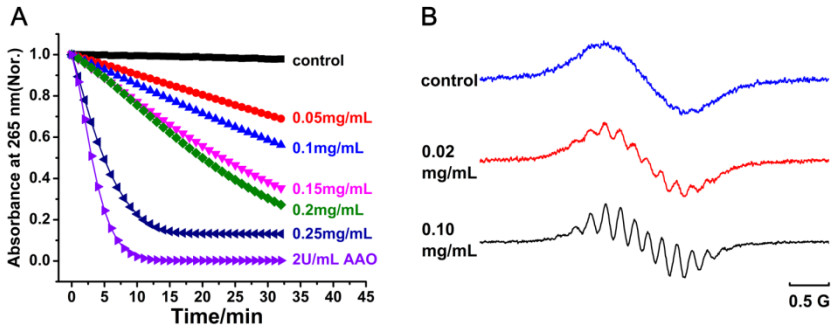


Fig. 5 Catalytic activity of Pd NPs during oxidation of AA. (A) AA absorbance at 265 nm as a function of time with different concentrations of Pd NPs. UV-Vis spectra for solutions of NPs with 0.25 mM AA in 10 mM PBS (pH 7.4). (B) ESR spectra for samples containing CTPO and different concentration of Pd NPs after mixing 5 min. The concentrations are: [CTPO] = 100 μM, [AA] = 5 mM, and [PBS] = 10 mM.

signal reduction exhibits a concentration-dependence at low mass concentrations (Fig. 4B). For Au@Pd NRs, they also show a similar dose-dependent scavenging effect. And they have a higher scavenging effect than Au NRs (Fig. S10†). Our results indicate that, when not exposed to light (i.e., excluding light in the SPR spectral range), Pd NSs actually scavenge $^1O_2$.

$^1O_2$ can significantly and quite often elicit undesirable consequences including cytotoxicity and/or disease development. Due to their bilateral influences with $^1O_2$ under different condidtions, Pd NSs may be useful as an effective means to regulate the levels of $^1O_2$ in cells.

From the viewpoint of ROS, Pd NSs show duality. On the one hand, they possess the advantages of scavenging superoxide radicals and singlet oxygen, decomposing $H_2O_2$ to dioxygen under neutral and alkaline conditions. On the other hand, they can facilitate the formation of highly reactive hydroxyl radicals during decomposition of $H_2O_2$ under strongly acidic conditions and thus may impose a negative biological effect. Based on the interactions between Pd NSs and ROSs, we propose a Fenton-like reaction and catalase-like catalytic activity might be responsible for the generation of •OH and $O_2$ in the presence of $H_2O_2$. However, the mechanisms for scavenging superoxide radicals and singlet oxygen are much complex and need further researches.

A number of endogenous and exogenous antioxidants are important for protecting organisms against oxidative damage. As Pd NPs also show oxidase-like activity, they may affect these antioxidants. Therefore, we examined interactions between Pd NPs and the biologically important antioxidant, ascorbic acid.

**Catalytic activity of Pd NSs during oxidation of Ascorbic acid (AA)**

As an often employed antioxidant, ascorbic acid (AA), can be oxidized slowly to the ascorbyl radical (AA•) (Fig. S11A†) by dioxygen. The presence of ascorbic acid oxidase (AAO) greatly accelerates this process (Fig. S11B†). We used the absorbance change of AA at ca. 265 nm to monitor its oxidation. As shown in Fig. 5A, Pd NPs obviously accelerate the oxidation of AA in dose-dependent manner.

The ESR spectrum of the spin probe CTPO exhibits three lines because of the hyperfine interaction between the unpaired electrons of oxygen and the nitrogen nucleus. Each line is further split into another group of lines because of proton superhyperfine interaction. The resolution of the superhyperfine structure of the low-field line of the ESR spectrum of CTPO depends on the oxygen concentration of the sample solution.[40] Thus, CTPO is commonly used for detecting changes in the concentration of oxygen. As Fig. 5B shows, at the same incubation time, the ESR spectrum of CTPO in the sample containing Pd NPs has more superhyperfine splitting than the control sample, indicating more consumption of oxygen. A more dramatic increase in superhyperfine splitting is observed for the sample containing high concentration of Pd NPs. This indicates substantial catalytic activity, consistent with results in Fig. 5A.

In previous reports, Au@Pt NRs and Au@Pd NRs have been found to catalyze the oxidation of AA by $O_2$.[41, 42] Here, we also observed the same effect of Au@Pd NRs on AA, however, Au NRs have negligible catalytic activity in the same concentration range (Fig. S11A†). This result consistents with the consumption of oxygen from ESR spectrum of CTPO (Fig. S11B†). The oxidase-like activity was also demonstrated using another molecule, CPH, as shown in Fig. S13†.

Oxidative stress is thought to be involved in the development of many diseases.[43] Oxidative stress results from

an imbalance between the production of ROS and a biological system's ability to readily detoxify the reactive intermediates or repair the resultant damage. Therefore, the effects of nanomaterials on cells or organisms should be considered from two perspectives: prooxidant and antioxidant. On one

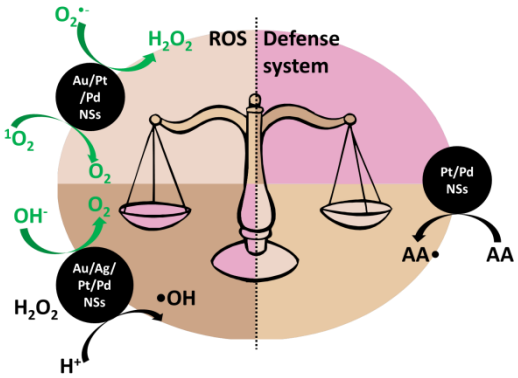


Scheme 1. Possible effects of noble metal nanostructures on ROS and the antioxidant defense system of organisms: two sides of the catalytic activities.

hand, we observed that Pd NSs can induce the generation of harmful hydroxyl radicals in the presence of $H_2O_2$ in a pH-dependent manner. And they may also catalyze the oxidation of antioxidants and reduce their protective role. These activities may challenge the antioxidant defenses of a cell or organism. On the other hand, Pd NSs can scavenge superoxide and singlet oxygen in ambient environment and thus play a positive role in controlling these two ROS.

Scheme 1 shows the activities of noble metal nanostructures on ROSs. Our results with Pd NSs along with previous reports on Au, Ag, and Pt, demonstrate that these four noble metal NSs all have similar pH-dependent catalytic behaviour during decomposition $H_2O_2$, i.e., generating hydroxyl radicals in strongly acidic conditions and producing $O_2$ in neutral and alkaline conditions. This common behaviour is in agreement with theoretical simulations.[19] Au, Pt and Pd NPs can scavenge superoxide and singlet oxygen. Pd and Pt NSs also have obvious impacts on antioxidants (such as AA).

## Conclusions

In summary, Pd NPs show some catalytic behaviours in generation and scavenging of ROS species similar to other noble metal nanomaterials, i.e., Au, Ag and Pt NPs. Using ESR coupled with spin trapping and spin labelling techniques, we demonstrate that Pd NSs (both Pd NPs and Au@Pd NRs) can induce $O_2$ and •OH production in the presence of $H_2O_2$. Oxygen is produced under neutral and alkaline conditions and •OH under acidic conditions. From the viewpoints of reducing ROS, Pd NSs could provide protective roles to biological systems at physiological pH owing to their scavenging effects on superoxide and singlet oxygen. Similar to Au NPs, Au NRs also show the same effects on ROS based on the results of this study. On the other hand, their oxidase-like activity can accelerate the oxidation of antioxidants and may produce negative biological effects. Here we systematically investigate the role of Pd NSs on ROS with experiments, and summarizes an overview of the role of noble metal nanostructures on ROS. Therefore, before employing noble metal nanostructures for biomedical applications, their effects under physiological relevant conditions need to be investigated.

## Acknowledgements

The work was supported by the National Natural Science Foundation of China (Grant No. 21173056) and partially supported by a regulatory science grant under the FDA Nanotechnology CORES Program. We are also grateful to Wayne G. Wamer (the Center for Food Safety & Applied Nutrition/US FDA) for his significant input in this study. This article is not an official U.S. FDA guidance or policy statement. No official support or endorsement by the U.S. FDA is intended or should be inferred.

## References

1 B. Woodward, *Platinum Met. Rev.*, 2012, **56**, 213-217.
2 C. P. Adams, K. A. Walker, S. O. Obare and K. M. Docherty, *PLoS One*, 2014, **9**, e85981.
3 A. Balbin, F. Gaballo, J. Ceballos-Torres, S. Prashar, M. Fajardo, G. N. Kaluderovic and S. Gomez-Ruiz, *RSC Adv.*, 2014, **4**, 54775-54787.
4 M. Liu, Y. Zheng, L. Zhang, L. Guo and Y. Xia, *J. Am. Chem. Soc.*, 2013, **135**, 11752-11755.
5 Y. Xiong, B. Wiley, J. Chen, Z. Y. Li, Y. Yin and Y. Xia, *Angew. Chem. Int. Ed.*, 2005, **44**, 7913-7917.
6 X. Huang, S. Tang, J. Yang, Y. Tan and N. Zheng, *J. Am. Chem. Soc.*, 2011, **133**, 15946-15949.
7 X. Huang, S. Tang, X. Mu, Y. Dai, G. Chen, Z. Zhou, F. Ruan, Z. Yang and N. Zheng, *Nat. Nanotechnol.*, 2011, **6**, 28-32.
8 Y. Wang, S. Xie, J. Liu, J. Park, C. Z. Huang and Y. Xia, *Nano Lett.*, 2013, **13**, 2276-2281.
9 H. Zhang, M. Jin, Y. Xiong, B. Lim and Y. Xia, *Acc. Chem. Res.*, 2013, **46**, 1783-1794.
10 A. Dumas and P. Couvreur, *Chem. Sci.*, 2015, **6**, 2153-2157.
11 H. Ohde, C. M. Wai, H. Kim, J. Kim and M. Ohde, *J. Am. Chem. Soc.*, 2002, **124**, 4540-4541.
12 S. Tang, M. Chen and N. Zheng, *Nano Res.*, 2015, **8**, 165-174.
13 L. Nie, M. Chen, X. Sun, P. Rong, N. Zheng and X. Chen, *Nanoscale*, 2014, **6**, 1271-1276.
14 M. Chen, S. Tang, Z. Guo, X. Wang, S. Mo, X. Huang, G. Liu and N. Zheng, *Adv. Mater.*, 2014, **26**, 8210-8216.
15 S. Tang, X. Huang and N. Zheng, *Chem Commun (Camb)*, 2011, **47**, 3948-3950.
16 A. Manke, L. Wang and Y. Rojanasakul, *Biomed Res. Int.*, 2013, **2013**, 942916.
17 N. Li, T. Xia and A. E. Nel, *Free Radical Biol. Med.*, 2008, **44**, 1689-1699.
18 J. C. Bonner, *Toxicol. Pathol.*, 2007, **35**, 148-153.
19 J. Li, W. Liu, X. Wu and X. Gao, *Biomaterials*, 2015, **48**, 37-44.
20 M. Chiesa, E. Giamello and M. Che, *Chem. Rev.*, 2010, **110**, 1320-1347.
21 Z. Wang, W. Ma, C. Chen, H. Ji and J. Zhao, *Chem. Eng. J.* , 2011, **170**, 353-362.

22 W. He, Y. T. Zhou, W. G. Wamer, X. Hu, X. Wu, Z. Zheng, M. D. Boudreau and J. J. Yin, *Biomaterials*, 2013, **34**, 765-773.
23 W. He, Y. T. Zhou, W. G. Wamer, M. D. Boudreau and J. J. Yin, *Biomaterials*, 2012, **33**, 7547-7555.
24 Y. Liu, H. Wu, M. Li, J.-J. Yin and Z. Nie, *Nanoscale*, 2014, **6**, 11904-11910.
25 K. Zhang, Y. Xiang, X. Wu, L. Feng, W. He, J. Liu, W. Zhou and S. Xie, *Langmuir*, 2009, **25**, 1162-1168.
26 J. J. Yin, F. Lao, P. P. Fu, W. G. Wamer, Y. Zhao, P. C. Wang, Y. Qiu, B. Sun, G. Xing, J. Dong, X. J. Liang and C. Chen, *Biomaterials*, 2009, **30**, 611-621.
27 H. Zhao, J. Joseph, H. Zhang, H. Karoui and B. Kalyanaraman, *Free Radical Biol. Med.*, 2001, **31**, 599-606.
28 K. Stolze, N. Udilova and H. Nohl, *Free Radical Bio. Med.*, 2000, **29**, 1005-1014.
29 G. M. Rosen, P. Tsai, J. Weaver, S. Porasuphatana, L. J. Roman, A. A. Starkov, G. Fiskum and S. Pou, *J. Biol. Chem.*, 2002, **277**, 40275-40280.
30 R. Vankayala, A. Sagadevan, P. Vijayaraghavan, C. L. Kuo and K. C. Hwang, *Angew. Chem.*, 2011, **50**, 10640-10644.
31 C. Jiang, T. Zhao, P. Yuan, N. Gao, Y. Pan, Z. Guan, N. Zhou and Q. H. Xu, *ACS Appl. Mater. Interfaces*, 2013, **5**, 4972-4977.
32 R. Vankayala, C. L. Kuo, A. Sagadevan, P.-H. Chen, C.-S. Chiang and K. C. Hwang, *J. Mater. Chem. B*, 2013, **1**, 4379-4387.
33 H. Kawasaki, S. Kumar, G. Li, C. Zeng, D. R. Kauffman, J. Yoshimoto, Y. Iwasaki and R. Jin, *Chem. Mater.*, 2014, **26**, 2777-2788.
34 L. Gao, R. Liu, F. Gao, Y. Wang, X. Jiang and X. Gao, *ACS Nano*, 2014, **8**, 7260-7271.
35 R. Long, K. Mao, X. Ye, W. Yan, Y. Huang, J. Wang, Y. Fu, X. Wang, X. Wu, Y. Xie and Y. Xiong, *J. Am. Chem. Soc.*, 2013, **135**, 3200-3207.
36 R. Long, K. Mao, M. Gong, S. Zhou, J. Hu, M. Zhi, Y. You, S. Bai, J. Jiang, Q. Zhang, X. Wu and Y. Xiong, *Angew. Chem. Int. Ed.*, 2014, **53**, 3205-3209.
37 Y. Yamamoto, N. Imai, R. Mashima, R. Konaka, M. Inoue and W. C. Dunlap, *Methods Enzymol.*, 2000, **319**, 29-37.
38 Y. Lion, M. Delmelle and A. Van De Vorst, *Nature*, 1976, **263**, 442-443.
39 J. Moan and E. Wold, *Nature*, 1979, **279**, 450-451.
40 C.-S. Lai, L. E. Hopwood, J. S. Hyde and S. Lukiewicz, *Proc. Natl. Acad. Sci.*, 1982, **79**, 1166-1170.
41 Y.-T. Zhou, W. He, W. G. Wamer, X. Hu, X. Wu, Y. M. Lo and J.-J. Yin, *Nanoscale*, 2013, **5**, 1583-1591.
42 K. Zhang, X. Hu, J. Liu, J.-J. Yin, S. Hou, T. Wen, W. He, Y. Ji, Y. Guo, Q. Wang and X. Wu, *Langmuir*, 2011, **27**, 2796-2803.
43 C. Gorrini, I. S. Harris and T. W. Mak, *Nat. Rev. Drug. Discov.*, 2013, **12**, 931-947.